Scanning Electron Microscopic Study of Microstructure of Gala Apples during Hot Air Drying

H. C. P. Karunasena [a, b], P. Hesami [a], W. Senadeera [a*], Y. T. Gu [a], R. J. Brown [a] and K. Oloyede [a]

[a] School of Chemistry Physics and Mechanical Engineering,
Faculty of Science and Engineering, Queensland University of Technology,
2, George Street, Brisbane, QLD - 4001, Australia.

[b] Department of Mechanical and Manufacturing Engineering, Faculty of Engineering,
University of Ruhuna, Hapugala, Galle, Sri Lanka.

[*] Corresponding author. Tel.: +61-7-3138 6887; Fax: +61-7-3138 1516
E-mail address: w3.senadeera@qut.edu.au

ABSTRACT

Microscopic changes occur in plant food materials during drying significantly influence the macroscopic properties and quality factors of the dried food materials. It is very critical to study microstructure to understand the underlying cellular mechanisms to improve performance of the food drying techniques. However, there is very limited research conducted on such microstructural changes of plant food material during drying. In this work, Gala apple parenchyma tissue samples were studied using a scanning electron microscope for gradual microstructural changes as affected by temperature, time and moisture content during hot air drying at two drying temperatures: 57 ℃ and 70 ℃. For fresh samples, the average cellular parameter values were; cell area: 20000 μm^2, ferret diameter: 160 μm, perimeter: 600 μm, roundness: 0.76, elongation: 1.45 and compactness: 0.84. During drying, a higher degree of cell shrinkage was observed with cell wall warping and increase in intercellular space. However, no significant cell wall breakage was observed. The overall reduction of cell area, ferret diameter and perimeter were about 60%, 40% and 30%. The cell roundness and elongation showed overall increments of about 5% and the compactness remained unchanged. Throughout the

drying cycle, cellular deformations were mainly influenced by the moisture content. During the initial and intermediate stages of drying, cellular deformations were also positively influenced by the drying temperature and the effect was reversed at the final stages of drying which provides clues for case hardening of the material.

Keywords: Food Drying; Microstructure; Plant cells; Scanning electron microscope; Cell deformations; Shrinkage

INTRODUCTION

Drying is used as a preservation technique for around 20% of the world's perishable crops[1]. By nature, plant food materials are highly susceptible to biological spoilage due to the higher water content[2] which can be as high as 90% on wet basis[3]. When the plant food materials are dried, preservation is mainly achieved by a significant moisture removal which directly influences to reduce biological reactions that cause spoilage. Due to such removal of moisture from food structures, significant bulk level and microstructural deformations occur which are very critical for quality controlling and process optimization in food engineering. Investigations on causes and effects of drying on such bulk level deformations are quite frequently reported as theoretical[4-9] and experimental[10-13] findings. These bulk level phenomena are interrelated with microscopic changes in the cell level[14-21] and the latter can be used to better explain such bulk level deformations. However, compared to the number of bulk level studies, only a handful of microstructural studies are available on drying of plant food materials both theoretically[22] and experimentally[14-18, 23-29]. This paper aims to fill this gap by visualizing and quantifying the cellular structural changes of plant tissues during drying with the assistance of a powerful microscopic technique: scanning electron microscopy.

Several authors have reported that cellular level deformations are mainly driven by the moisture content of the plant tissue[10, 14-18, 26, 30-34], drying temperature[10, 12, 13] and the cell turgor pressure[35]. In the recent past, apple fruit has been a common subject for drying experiments mainly due to its industrial importance[19-21, 27]. In fresh apple tissues, cells are densely packed[30] and they tend to shrink considerably during drying[14, 18] without much cell wall breakage[16, 25, 30] which is mainly due to the rigid skeleton like structure[36]. Further, the intercellular bonds tend to become loose during drying and cells can gradually separate from each other[37, 38]. To characterise these kinds of complex structural deformations, many geometrical parameters are defined for cells such as: two-dimensional area (*A*), ferret diameter[1] (*D*), perimeter (*P*), roundness[2] (*R*), elongation[3] (*EL*) and compactness[4] (*C*). In fresh samples, these parameter values tend to differ mainly based on the cultivar and the level of maturity. Such parameter values found in literature data for different apple fruit cultivars are given in Table 1.

Apart from these cell measurements, several previous authors have reported that about 25% of the fresh tissue volume is composed of intercellular spaces[39-43] and mostly they are spherical in three-dimensional shape[44]. Their two-dimensional area can be about 83000 μm^2 for golden Delicious apples[18], the ferret diameter can range from 90 - 140 μm[41] and even be as large as 320 μm[18]. The perimeter is about 1230 μm[18]. The shape parameters for intercellular spaces of golden Delicious apples are; roundness: 0.7, compactness: 0.74 and elongation: 1.81[18]. These imply that the intercellular spaces have quite similar geometric parameters as cells. Also during drying, both plant cells and intercellular spaces experience quite similar shrinkage trends when considering the cell

[1] $\sqrt{4A/\pi}$
[2] $4\pi A/P^2$
[3] major axis length / minor axis length
[4] $\sqrt{4A/\pi}$ /(major axis length)

area, ferret diameter and perimeter reductions[16, 18, 30]. Also the cell roundness and elongation increments are found to be comparable[18, 24] as is the compactness[18].

In this background, the aim of our study was to visually analyse the morphological changes of apple cell structure and to quantify different cellular shape parameters as influenced by drying temperature, drying time and moisture content. Based on the details given above, we focused much on the overall cell structure in this study and studied the deformations characterised by the cell boundaries which would represent the overall deformations of the cell structure. Also, we selected the Gala apple cultivar for our investigation as it has not yet been subjected to such a detailed microscopic study in this regard. By considering the industrial importance and the comparability with the literature data, drying experiments were conducted at two selected temperatures: 57 ℃ and 70 ℃. We believe these findings will be quite useful for the scientific community who are interested in modelling such trends numerically[45-48] as well as for those who are interested in further experimental investigations.

MATERIALS AND METHODS

Material and sample preparation

For this study, Gala apples obtained from a local supermarket in the Brisbane - Australia were used. The average wet basis moisture content (X_{wet}) of the apples was 0.84 ± 0.01 and were kept stored at 4 ℃ before processing. Then the apples were washed in water and peeled by using a sharp knife. Next, with the use of sharp edged cylindrical cutting tools, ring shaped slices of 60 mm outer diameter, 25 mm inner diameter and 10 mm thickness were obtained from the middle parenchyma region of the fruit. To prevent enzymatic browning, these were pre-treated with 3% citric acid solution at 20 ℃ for 1 minute.

Drying experiments

Above processed samples were dried in a convective air dryer (Excalibur's 5-tray dehydrator - USA) which consists of an electric heater and a fan to produce a uniform hot air flow through the samples. Additionally, it has a thermostat to control the hot air temperature and a timer to control the drying time. From the five trays of the dryer, we used only the middle one and therefore removed the remaining trays. A constant horizontal air velocity of 1.5 ms^{-1} was always maintained during the drying experiments and two sets of drying studies were conducted by maintaining the air temperature at 57 ℃ and 70 ℃. In each set of drying studies, independent samples were used and dried individually for 30, 60, 90, 120, 150, 180 and 210 minutes. At the end of each individual drying cycle, the samples were taken out and cooled in a desiccator. A small sized desiccator was used for this purpose and no desiccant was used inside to ensure no significant level of further drying happens to the samples during the cooling time. Thereafter, one half of the sample was used for moisture content measurements in each case and the other half was used for microstructural investigations.

Moisture content measurements

For moisture content determination, standard AOAC method 934.06 (1995) as suggested by several authors could not be performed due to the absence of a vacuum pump to obtain necessary 13.3 kPa vacuum. Instead, a weight based method was used. Firstly, prior to drying experiments, weights of the fresh samples were measured using a digital weighing scale (Electrical balance B/C series – Germany). Next, one half of the samples were taken after each of the drying experiment and the weights were measured. Then, each of these samples were secondary dried at 100 ℃ in an oven (Heraeus RT 360 - Germany) and weights were recorded in every 0.5 hours time intervals. The drying process was continued until the samples were completely dried such that the difference

between the last two consecutive weight measurements was less than 0.1 mg. The average time taken for this complete drying phase was about 18 hours. Finally, X_{wet} and dry basis moisture content (X) were calculated for each case using the weight measurements.

Sample preparation for microstructural examination

As mentioned above, one half of the hot air oven dried samples in each case were taken for microstructural examination and were initially cut in to cubic specimens of 10 mm × 5 mm × 5 mm by using a sharp knife. These were initially coated with a fixative solution containing 2.5% glutaraldehyde, 4% paraformaldehyde, and 0.1 M cacodylate buffer (pH 7.2) and stored at 4 ℃ for about 12 hours. Then 0.1 M cacodylate buffer (pH 7.4) was used to rinse the samples before post fixing with cacodylate-buffered 1% osmium tetroxide for 4 hours in room temperature. Then, the samples were dehydrated using ethanol solutions of incremental concentrations of 50%, 70% and 90% twice for 10 minutes in each case. Next, the samples were dehydrated once in a 100% ethanol solution for 10 minutes. These dehydrated samples were then dried twice for 30 minutes using a Critical Point Drying[49, 50] apparatus (Tousimis Autosamdri-815 - USA). These prepared samples were fractured by freezing in liquid Nitrogen to obtain fresh cut sections for microscopic examinations. This method of fracturing helps to avoid any undesirable distortions that can appear on the tissue surface if any mechanical fracturing methods are involved. Then, the samples with such fresh-open cross-sections were mounted on metal stubs with double sided carbon tape followed by sputter coating up to10 µm of gold using an automated sputter coater (Leica EM SCD005 - Austria).

Scanning electron microscopy (SEM)

The above prepared samples were then examined by using a scanning electron microscope (FEI Quanta 200 Environmental) at 20 kV. In each case, the samples were

observed at the centre along the cross-section and imaged at 200× magnification with image size of 885 × 1022 pixels (1 pixel = 1.25 μm × 1.25 μm).

Image analysis

In our study, independent tissue samples were used for each experiment (as discussed above) to avoid possible measurement errors and experimental difficulties. Because of this, the same cells were not observed for gradual structural changes during a complete drying cycle (in our study: 210 minutes of drying). Instead, each individually dried sample was used for corresponding SEM imaging followed by image analysis using the ImageJ software (version 1.46). Each obtained tissue image was firstly black and white-converted and divided to small sub-regions such that each includes a single cell. Next, each small region was processed with noise filtering, smoothing and then subjected to edge detection to identify the cell walls. Then, the area measurement facility was used to quantify the pixel area bounded by the cell wall. This was then converted to actual dimensions by the use of the scale available in each SEM image. At the same time, the software facilitates to quantify many other geometric parameters corresponds to the particular cell such as ferret diameter, perimeter, roundness, elongation and compactness. Similarly, for a given tissue sample, all the sub-regions were processed and finally the overall representative average cell area (A), ferret diameter (D), perimeter (P), roundness (R), elongation (EL) and compactness (C) values were quantified. The averaging was done without filtering whether the measurements corresponded to actual cells or intercellular spaces[30]. This approach seems to be acceptable since many authors have reported that the cells and intercellular spaces have quiet similar geometries and shrinkage behaviours during drying as discussed above. However, some authors[18] have used a cell area-based method to generally sort-out the cells and intercellular spaces in the samples. Considering the biological variability of the cells and intercellular spaces, we

believe that it is quite difficult and not sufficiently accurate to define such a global cell size range to filter-out actual cells. Also if such an approach is used, it needs to be consistently followed for all the dried samples and it would be a very formidable task as both of the cells and intercellular spaces tend to shirk during drying. Also, there is a higher possibility to misinterpret shrunken intercellular spaces as cells or vice versa. So, the whole structure was considered in this study and measurements were done without distinguishing between cells and intercellular spaces.

RESULTS AND DISCUSSION

Drying kinetics

As seen from Fig. 1, for both of the temperatures that were studied, the constant rate drying period can't be clearly identified[51] which may principally exists in the very early stage of drying (< 30 minutes). But the falling rate drying period (< 150 minutes) is clearly observed and finally, both of the samples reach steady state moisture contents at extremely dried conditions (150 – 210 minutes). The higher drying temperature (70 ℃) causes samples to attain the equilibrium moisture state slightly earlier (after about 180 minutes), compared to the 57 ℃ drying which takes about 210 minutes. When compared with the curve of literature data[18], moisture content has reduced rapidly during our drying processes which may be mainly due to the forced convection method which was used that involves higher air velocities[52] rather than the natural convection based oven drying that these particular authors have used. Also, their drying curve exhibits some extended constant rate drying period (0 – 60 minutes) followed by falling rate periods, which reconfirms the slower moisture removal behaviour in their experiments.

When we further analyse the 57 ℃ and 70 ℃ curves in Fig. 1, different localized trends can be identified which could be related to the temperature influence for the drying process. Until about 30 minutes, there is a clear positive influence from the drying

temperature for the moisture removal rate. This should be due to the quick evaporation of moisture mainly from the material surface with the influence of the higher drying temperature[53] which basically acts as an external factor for drying[54]. During this initial stage, internal moisture of the food material tends to diffuse towards external surfaces and get evaporated to the hot air flow. Within the 30 - 60 minutes time interval, the observed drying rates of 57 ℃ and 70 ℃ seem to be quite similar. This should be due to the reduction of the internal moisture transfer rate as a result of the increased internal resistance for moisture diffusion during the falling rate period[54]. This effect is comparatively dominant in the case of the higher drying temperature which may be due to the comparatively lower level of absolute moisture content existing in the interior of those samples by that time. This effect is further observed during 60 - 90 minutes time interval where the drying rate of the 57 ℃ curve exceeds rate of 70 ℃ curve, implying that the 57 ℃ drying samples are still having comparatively lower resistance to the internal moisture transfer. During 90 - 150 minutes, the drying rate of 57 ℃ curve mostly remains constant while 70 ℃ curve experiences a slight increment followed by a decrement. However, the average moisture removal rate of the 57 ℃ curve is still slightly higher within this particular time period. This again implies that the lower temperature drying samples are having a comparatively lower internal resistance for the moisture transfer during these intermediate stages of drying. This should be mainly due to the comparatively higher moisture content and limited structural alterations to restrict the moisture transfer. The same effect is repeatedly observed even at the latter part of the experiments (150 - 210 minutes). However, the difference is fairly lower compared to the previous stages. This implies that the internal moisture contents of both the samples are reaching a minimum level, independent of the drying temperature.

Microstructural changes

The SEM images obtained from the drying experiments conducted at 57 ℃ and 70 ℃ are presented in Fig. 2 and Fig. 3, respectively. In fresh tissues as seen from Fig. 2(a) and Fig. 3(a), the majority of the cells are quite similar in sizes while some are comparatively smaller or larger. They generally seem to be circular in two-dimensional shape which is mainly due to the equilibrium of cell fluid turgor pressure forces and the cell wall tension[30, 55-60]. When tissues get dried, a significant microstructural deformation happens as seen from Fig. 2(b) - (h) and Fig. 3(b) - (h) which is mainly driven by the moisture removal from the cell fluid followed by the turgor loss. Response of cell walls to the turgor loss can be broadly defined based on two stages. Firstly, as the turgor pressure tends to decrease with drying, cell wall becomes less stretched and as a result, overall cellular dimensions get reduced. But, with respective to the atmosphere, since there is a significant positive turgor pressure inside the cell, its shape tends to remain fairly circular throughout this stage. Also in the meantime, there can be contractions of the cell walls due to the influence of drying, which can contribute to area, diameter and perimeter reductions of individual cells. As the drying is continued further, the cell fluid get further removed while the turgor pressure would reach a minimum. In this second stage, the cell wall will have a very lower tension and will undergo higher degree of warping and wrinkling to accommodate lower cell fluid volumes. Such cellular deformations are extensive and irregular as seen from Fig. 2(d) - (h) and Fig. 3(d) - (h). Due to these microscale contractions, volume of voids tend to increase in the material during drying, which mainly leads to increased bulk porosity and reduced bulk density. Further, since the plant cells usually have rigid cell walls, above microscale deformations are restrained at some degree and it is observed that the cell walls seem to undergo minimum destruction during drying.

Other than these effects of individual cell deformations, intercellular spaces also play an important role in microstructural deformations. Compared to the densely packed fresh cell structures seen from Fig. 2(a) and Fig. 3(a), the dried cell structures seen in Fig. 2(g), Fig. 2(h), Fig. 3(g) and Fig. 3(h) seem to have loosely bonded cells which can be observed from the expanded and newly formed intercellular spaces. These may be mainly due to the removal of moisture in these regions and expansion of entrapped air and vapour. Further, when the effect of drying temperature is considered, the two temperatures used in this work were found to be producing quite similar dried tissue structures. This may be due to the non-significant difference of the selected two drying temperatures in this experiment. However, in case if much higher drying temperatures were used, higher degree of expansions and formations of the intercellular spaces could be expected which would lead to increased bulk porosity and reduced bulk density of the food material.

To further study the cellular level geometric changes, several geometric parameters were quantified using image analysis as discussed above and the numerical results are presented in Table 2, Table 3 and their trends are graphically presented in Fig. 4 to Fig. 9. From Table 2 and Table 3, the average fresh cell area is found to be in the range of 20,000 μm^2 with standard deviation about 40% of the average area value. This indicates a higher degree of cell area variability in fresh apple tissues. The gala apple cells that we studied seem to be in the same size range compared to the golden Delicious, Braeburn and Jonagored apple varieties as seen from Table 1. During drying, the cell area variability only slightly reduces to about 30% which indicates that independent of the cell sizes, all cells experience similar area shrinkage. This trend is equally observed in both of the drying temperatures and eventually the extremely dried cell areas are in the range of 8500 μm^2 for both cases. In fresh samples, the average cell ferret diameter is about 160 μm, which is comparable with Delicious, golden Delicious, Braeburn and Jonagored

apple varieties. In our experiments, with the influence of drying, the cell diameter reduces to about 100 μm in both of the drying temperatures and the reduction is about 36%. Compared to cell area trends, the diameter variation in each instance is lower and remains within the range 12% to 20%. The average cell perimeter of fresh cells is observed to be about 600 μm with standard deviation about 14%, and is comparable with golden Delicious, Braeburn and Jonagored apple verities. In the latter part of the drying cycle, the cell perimeter reduces to about 375 μm with standard deviation about 21%.

Next, when the cell roundness is considered, fresh cells have 0.727 of average roundness with 18% standard deviation. This indicates that the fresh cells are not quite circular in two-dimensional shape. These values are well within the range of previous findings for golden delicious and Idared apples as mentioned above. The average roundness of dried samples is about 0.76 at 57 ℃ and 70 ℃ with standard deviation of 13% and 9%, respectively. This is comparable with values of dried golden Delicious apple cells: 0.68 [18] but comparatively higher than the values of Idared apples: 0.6[30]. When comparing the average roundness values for tissues, dried samples seem to have slightly higher roundness compared to fresh samples which opposes what can be expected if individual circular shaped cells were dried. The main reason for such a different trend in tissues can be the generation and expansion of circular shaped intercellular voids during the final stage of the drying cycle. These voids mostly have similar dimensions compared to the shrinked cells (see Fig.2 (h) and Fig. 3(h)) and it is quite difficult to distinguish and avoid when taking the average of the cell roundness for tissues. So, higher overall average roundness values can be expected. Also, since the standard deviation of roundness is about 20% for fresh cells and 10% for dried cells, actual roundness changes of individual cells can be different than this average trend. Further, since we have used different tissue samples to obtain different dried cell states, there can be some influence due the biological variability which results in these trends.

The average elongation of fresh cells is 1.459 and during drying, it increases slightly up to 1.52 and 1.6 at 57 ℃ and 70 ℃, respectively. The corresponding standard deviations are in the range 14% to 27%. Comparable dried cell elongation values such as 1.8 are reported for dried golden delicious apples[18]. The compactness remains almost constant throughout the drying cycle at both of the temperatures where it just changes from 0.84 in fresh cells to 0.83 and 0.81 at extremely dried states corresponding to 57 ℃ and 70 ℃ drying temperatures, respectively. The corresponding standard deviation variation is in the range of 8% to 14%, which is comparatively lower than in case of other geometrical parameters. Quite similar compactness values (0.77 - 0.82) are reported for dried cells of golden delicious apples[18].

In Fig. 4, the cell area trends are presented and as seen from Fig. 4(a), the normalized area trends are such that, as the drying progresses, the area reduces from 60% compared to the fresh condition. Such a higher degree of cell area reduction implies the extreme deformations that the cell structures undergo during drying. Further, it is seen that if the drying temperature is increased, the cell area reduction is accelerated at the initial stages of drying. But, eventually both of the drying temperatures seem to produce a similar overall cell area reduction at the end of drying. From Fig. 4(b), the lower temperature drying curve indicates that only 20% of the area reduction is observed even at about 80% of moisture reduction. Thereafter, the area reduces rapidly. From the higher temperature curve, a similar trend is observed, but with a higher degree of area reduction. The cell area reductions observed by other researchers seem to be comparable with our findings. Probability density functions (PDFs) of the cell area within each test case at 57 ℃ are presented in Fig. 4(c) and the most frequent fresh cell area observed is about 20,000 μm^2. It can be seen that the cell area of the fresh sample is distributed in a wide range and as the drying progresses, the mean area of cells tend to characterise lower values and the frequency of smaller cells in dried samples are higher compared to moisture rich samples.

In Fig. 4(d), a similar trend is observed for higher temperature, but with slightly broader distributions.

In Fig. 5, the cell ferret diameter variations are presented and as seen in Fig. 5(a), the fresh cell normalized ferret diameter curves show a decreasing trend throughout the drying cycle and finally, the cell diameter reaches lower values that are about 60% of the fresh cell diameter. In the case of higher drying temperature, the diameter reductions are relatively higher and the 70 ℃ curve is in good agreement with literature results of 70 ℃ drying[18]. In Fig. 5(b), both of the temperature curves indicate modest shrinkage until X/X_0 reaches about 0.1 and thereafter rapid reductions are observed. Trends shown in Fig. 5(c) indicate the most frequent fresh cell ferret diameter is about 160 μm. As the drying progresses, the mean cell ferret diameter gradually reduces and the most frequent dried cell ferret diameter is about 100 μm. As seen from Fig. 5(d), at the higher temperature (70 ℃), the ferret diameter values tend to have narrower distributions than in case of 57 ℃ and the most frequent extremely dried cell ferret diameter is about 100 μm.

Cell perimeter characteristics are presented in Fig. 6 and according to Fig. 6(a), the cell perimeter tends to reduce consistently as drying progresses and eventually reaches a minimum perimeter value which is about 70% of the fresh cell perimeter. As given in Fig. 6(b), when the perimeter trend is observed against the moisture content, for both of the temperatures, the cell perimeter follows an identical decreasing trend until the X/X_0 equals to 0.5. Thereafter a significant decrement is observed in the higher temperature curve. Further, as the drying progresses, independent of the drying temperature, the perimeter reduces slightly down to about 90% from its initial value until X/X_0 reaches about 0.1 and thereafter reduces quite rapidly. The literature data on perimeter reductions[18] are quite comparable with our results both in time and moisture domains. The variations of cell perimeter in each test case at lower temperature are presented in Fig. 4(c) and the most frequent fresh cell perimeter observed is about 600 μm and most frequent dried cell

perimeter is about 400 μm. From Fig. 4(d), for the higher temperature drying experiments, a similar trend is observed but with much narrower distribution, indicating that the cells tend to have quite uniform perimeter values in each dried sample.

When further studying Fig. 4 to Fig. 6, in case of extremely dried stages ($X/X_0 < 0.1$), deformation trends seems to be quite different that in case of higher moist stages. *Glass transition* is one of the key theoretical concepts used to explain this kind of shrinkage and collapse of food structures during drying[61-63], specially for freeze dried food materials[64]. It assumes that there can be significant shrinkage during drying only if the drying temperature is higher than the particular glass transition temperature of the material at that particular moisture content. However, for explaining shrinkage of convective air dried food materials, *case hardening* phenomenon is found to be more appropriate[12, 13, 65]. According to this phenomenon, when higher drying temperatures are used for drying, surface moisture tends to decrease rapidly and the outer tissue layers tend to get fairly dried quite earlier. Then, these outer tissues usually become more rigid to act as a hardened case which would resist further mass transfer from interior tissues to exterior tissues and eventually restrains the shrinkage of the material. But, in case if a lower drying temperature is used, the moisture removal happens comparatively slower but the mass transfer is fairly uniform across the material from centre to the outer layers. This facilitates continued moisture removal from the material throughout the drying cycle that eventually leads to a higher overall shrinkage. This has been clearly observed for apples during convective air drying[12, 25]. When referring to Fig. 4 – Fig. 6, this phenomenon is evident for extremely dried samples ($X/X_0 < 0.1$) where the 57 ℃ curves show much higher shrinkage behaviour than 70 ℃ curves. This provides clues for the existence of the case hardening phenomenon in extremely dried apple tissues. However, for high moist samples ($X/X_0 > 0.1$), the higher temperature usually tends to produce higher level of shrinkage which can be observed from Fig. 4 – Fig. 6. This may be related with the

structural collapse and contractions of the cell wall fibrous structure influenced by the moderately higher drying temperature and rapid moisture reduction.

Next, the cell roundness results are presented in Fig. 7 and as seen in Fig. 7(a), the normalized roundness values slightly increase during drying from about 5%, indicating that the cells deviate only slightly from their initial circular shapes. The drying temperature also seems to cause slight changes of the cell roundness trends in the intermediate stages of drying. However, the eventual normalized roundness values seem to be quite similar in both of the temperatures. Next, as seen in Fig. 7(b), when the roundness trends are studied against the moisture content, most of the rapid fluctuations are observed only at extremely dried cell states where the X/X_0 reduces beyond 0.1. However, considering both Fig. 7(a) and Fig. 7(b), the roundness values for Gala apples are slightly higher than the values obtained for golden delicious apples by previous authors[18], which provides clues of the cellular structural variability existing between different apple cultivars and their inherited deformation characteristics. Also, there can be some influence from the drying method used where we employed forced convection rather than the natural convection[18]. As seen from Fig. 7(c) and Fig. 7(d), the variations of cell roundness in both of the lower and higher temperature test cases indicate quite similar trends, which imply that the cells of dried samples frequently have similar roundness values. Also, the trends observed at the higher temperature are comparatively narrower, which imply that the drying temperature seems to positively influence on uniform cellular shrinkage and shape change.

In Fig. 8, the cell elongation trends are presented and as seen from Fig. 8(a), the normalized cell elongation slightly increases as the drying progresses and in the case of the higher temperature, the increment is about 10% and for the lower temperature it is about 5%. Both of the curves indicate similar local trends in the time domain but with different magnitudes. From Fig. 8(b), the elongation curves corresponding to both of the

temperatures reach their minimum values when X/X_0 is about 0.1 and rapidly increase thereafter. In case of the higher temperature curve, quite rapid fluctuations are observed when $X/X_0 < 0.04$. In Fig. 8(a) and Fig. 8(b), similar elongation trends are observed for Gala apples and golden Delicious apples[18]. As seen in Fig. 8(c) and Fig. 8(d), the variations of cell elongation in both of the temperatures do not indicate significant differences, implying similar cell elongation variations of cells at both of the drying temperatures.

Cell compactness trends are presented in Fig. 9 and when considering both of the time domain trends (Fig. 9(a)) and moisture content domain trends (Fig. 9(b)), the cell compactness remains almost equal to 1.0 which is in good agreement with the findings of other researchers[18]. In these results, only a slight positive influence of the drying temperature is observed on the cell compactness. Also, as seen from Fig. 9(c) and Fig. 9(d), the variations of cell compactness are quite similar implying that the, independent of the drying temperature, cell compactness variation remains almost unchanged during drying.

CONCLUSIONS

A detailed SEM-based microscopic study has been conducted on Gala apple parenchyma cells to study their structural deformations during convective air drying as influenced by drying temperature, drying time and moisture content. The results have been presented qualitatively with microscopic images and quantitatively using image analysis on several geometric parameters.

Specifically, we have found:

- Fresh cells of gala apple parenchyma region exist in a densely packed structure and during drying, their interconnections become lose which is observed by the

increased number and sizes of intercellular spaces. Also, the cells undergo excessive deformations during drying and the cell walls tend to experience higher degree of warping and wrinkling, but without much significant cell wall destructions.

- When considering the whole drying cycle, about 80% of the moisture got removed within the initial 30% of the drying cycle (60 minutes) and the temperature positively influences the rate of moisture removal. Thereafter, the moisture removal rates at both of the drying temperature become fairly equal and at the latter part of the cycle, the lower temperature seems to produce slightly higher moisture removal rates. However, at the end of each drying cycle, independent of the drying temperature, the final dry basis moisture content attained was about 0.015.
- Average geometric parameters of fresh Gala apple cells are: 2-dimentional area: 20000 μm^2, ferret diameter: 160 μm, perimeter: 600 μm, roundness: 0.72, elongation: 1.45 and compactness: 0.84. In case of extremely dried Gala apple cells: two-dimensional area: 8600 μm^2, ferret diameter: 105 μm, perimeter: 370 μm, roundness: 0.76, elongation: 1.55 and compactness: 0.81.
- At the initial and intermediate stages of drying ($X/X_0 > 0.1$), the drying temperature positively influences the cell area reduction which can be mainly due to the rapid changes such as turgor pressure, cell wall contractions and collapse of tissue structures. However, at the extremely dried stages ($X/X_0 < 0.1$), due to the case hardening effects, higher drying temperature usually results in comparatively lower shrinkage characteristics which can be clearly observed in cell area, ferret diameter and perimeter trends.
- At the extremely dried conditions, the overall cell area reduction is about 60% which is independent of the drying temperature. For the initial half of this

reduction, about 80% of the total moisture content needs to be reduced. Compared to the fresh tissue samples, cell area variation is less in dried samples.

- During drying, the overall cell ferret diameter reduction is 40%, perimeter reduction is 30% and elongation increment is 5 - 10%. But the cell roundness and cell compactness mostly remain unchanged.
- As far as the final extremely dried conditions are considered, there were no significant influences of drying temperature on the cellular geometric parameters which may be due to the moderately higher temperature values used in this work and their non-significant difference.
- During drying, the changes of key shape parameters such as roundness, elongation and compactness were found to be comparable with most of the other apple cultivars although their cellular geometric parameters such as area, ferret diameter and perimeter were quite different.

To conclude, these findings and the data we present here will specially assist both the future experimental and numerical modelling researchers for comparison and validation of their works. The SEM method can be recommended as a powerful tool to visually investigate dried cells and tissues. However, it is difficult to keep focus on the same cell sample throughout the entire drying cycle. If such means are further explored in the future, it will help to reveal drying originated plant cell morphological changes in more detail. Further, when using moderately higher drying temperatures, the moisture content alone can be used to explain cell area and ferret diameter reductions during drying. But in case of cell perimeter reductions that were observed, both the moisture content and the turgor pressure are needed, since the cell wall perimeter reduction indicates some degree of wall contractions. So, to better understand the relationship between the turgor pressure and cell deformations, further experiments are recommended.

NOMENCLATURE

A	Cell top surface area (m^2)
A_0	Cell top surface area at fresh condition (m^2)
A/A_0	Normalized cell area
C	Cell compactness
C_0	Cell compactness at fresh condition
C/C_0	Normalized cell compactness
D	Cell ferret diameter (m)
D_0	Cell ferret diameter at fresh condition (m)
D/D_0	Normalized cell ferret diameter
EL	Cell elongation
EL_0	Cell elongation at fresh condition
EL/EL_0	Normalized cell elongation
P	Cell perimeter (m)
P_0	Cell perimeter at fresh condition (m)
P/P_0	Normalized cell perimeter
R	Cell roundness
R_0	Cell roundness at fresh condition
R/R_0	Normalized cell roundness
X	Dry basis moisture content (kg_{water} / $kg_{dry\ material}$)
X_0	Dry basis moisture content at fresh condition
X/X_0	Dry basis normalized moisture content
X_{wet}	Wet basis moisture content (kg_{water} / $kg_{wet\ material}$)

ACKNOWLEDGEMENTS

This research was conducted at the experimental facilities of the Queensland University of Technology (QUT) - Brisbane, Australia and the research studies were financially supported by QUT, International Postgraduate Research Scholarship (IPRS) and Australian Postgraduate Award (APA) scholarship. Support from the ARC Future Fellowship grant (FT100100172), high performance computer resources provided by the QUT and the overall support given by Faculty of Engineering, University of Ruhuna, Sri Lanka are also gratefully acknowledged.

REFERENCES

1. Grabowski, S., M. Marcotte, and H.S. Ramaswamy, *Drying of Fruits, Vegetables, and Spices* in *Handbook of postharvest technology : cereals, fruits, vegetables, tea, and spices*, A. Chakraverty, et al., Editors. 2003, Marcel Dekker: New York p. 653-695.
2. García, S.V., et al., *Influence of Drying Temperature on the Physical and Microbiological Parameters and the Quality of Dried Green Onion.* Drying Technology, 2010. 28(12): p. 1435-1444.
3. Jangam, S.V., *An Overview of Recent Developments and Some R&D Challenges Related to Drying of Foods.* Drying Technology, 2011. 29(12): p. 1343-1357.
4. Jan Kowalski, S., *Mathematical Modelling of Shrinkage During Drying.* Drying Technology, 1996. 14(2): p. 307-331.
5. Rossello, C., et al., *Simple mathematical model to predict the drying rates of potatoes.* Journal of Agricultural and Food Chemistry, 1992. 40(12): p. 2374-2378.

6. Simal, S., et al., *Heat and mass transfer model for potato drying.* Chemical Engineering Science, 1994. 49(22): p. 3739-3744.
7. Pabis, S., *Theoretical models of vegetable drying by convection.* Transport in Porous Media, 2007. 66(1): p. 77-87.
8. Rahman, M.S., *A Theoretical Model to Predict the Formation of Pores in Foods During Drying.* International Journal of Food Properties, 2003. 6(1): p. 61-72.
9. Golestani, R., A. Raisi, and A. Aroujalian, *Mathematical Modeling on Air Drying of Apples Considering Shrinkage and Variable Diffusion Coefficient.* Drying Technology, 2013. 31(1): p. 40-51.
10. Karathanos, V., *Collapse of structure during drying of celery.* Drying Technology, 1993. 11(5): p. 1005-1023.
11. Karathanos, V.T., N.K. Kanellopoulos, and V.G. Belessiotis, *Development of porous structure during air drying of agricultural plant products.* Journal of Food Engineering, 1996. 29(2): p. 167-183.
12. Wang, N. and J.G. Brennan, *Changes in structure, density and porosity of potato during dehydration.* Journal of Food Engineering, 1995. 24(1): p. 61-76.
13. Rahman, M.S., I. Al-Zakwani, and N. Guizani, *Pore formation in apple during air-drying as a function of temperature: porosity and pore-size distribution.* Journal of the Science of Food and Agriculture, 2005. 85(6): p. 979-989.
14. Lee, C.Y., D.K. Salunkhe, and F.S. Nury, *Some chemical and histological changes in dehydrated apple.* Journal of the Science of Food and Agriculture, 1967. 18(3): p. 89-93.
15. Hills, B.P. and B. Remigereau, *NMR studies of changes in subcellular water compartmentation in parenchyma apple tissue during drying and freezing.* International Journal of Food Science & Technology, 1997. 32(1): p. 51-61.

16. Lewicki, P.P.D., J. *Effect of drying on tissue structure of selected fruits and vegetables*. in *Proceedings of the 11th International Drying Symposium Drying 98*. 1998. Greece: Ziti Editions Thessaloniki.
17. Ramos, I.N., et al., *Quantification of microstructural changes during first stage air drying of grape tissue.* Journal of Food Engineering, 2004. 62(2): p. 159-164.
18. Mayor, L., M.A. Silva, and A.M. Sereno, *Microstructural Changes during Drying of Apple Slices.* Drying Technology, 2005. 23(9-11): p. 2261-2276.
19. Witrowa-Rajchert, D. and M. Rząca, *Effect of Drying Method on the Microstructure and Physical Properties of Dried Apples.* Drying Technology, 2009. 27(7-8): p. 903-909.
20. Han, Q.-H., et al., *Optimization of Process Parameters for Microwave Vacuum Drying of Apple Slices Using Response Surface Method.* Drying Technology, 2010. 28(4): p. 523-532.
21. Sabarez, H.T., J.A. Gallego-Juarez, and E. Riera, *Ultrasonic-Assisted Convective Drying of Apple Slices.* Drying Technology, 2012. 30(9): p. 989-997.
22. Crapiste, G.H., S. Whitaker, and E. Rotstein, *Drying of cellular material—I. A mass transfer theory*. Chemical Engineering Science, 1988-a. 43(11): p. 2919-2928.
23. Crapiste, G.H., S. Whitaker, and E. Rotstein, *Drying of cellular material—II. Experimental and numerical results.* Chemical Engineering Science, 1988-b. 43(11): p. 2929-2936.
24. Bolin, H.R. and C.C. Huxsoll, *Scanning Electron Microscope/Image Analyzer Determination of Dimensional Postharvest Changes in Fruit Cells.* Journal of Food Science, 1987. 52(6): p. 1649-1650.
25. Bai, Y., et al., *Structural Changes in Apple Rings during Convection Air-Drying with Controlled Temperature and Humidity.* Journal of Agricultural and Food Chemistry, 2002. 50(11): p. 3179-3185.

26. Lozano, J.E., E. Rotstein, and M.J. Urbicain, *Total porosity and open-pore porosity in the drying of fruits.* Journal of Food Science, 1980. 45(5): p. 1403-1407.
27. Chen, X.D., et al., *In Situ ESEM Examination of Microstructural Changes of an Apple Tissue Sample Undergoing Low-Pressure Air-Drying Followed by Wetting.* Drying Technology, 2006. 24(8): p. 965-972.
28. Ong, S.P. and C.L. Law, *Microstructure and Optical Properties of Salak Fruit Under Different Drying and Pretreatment Conditions.* Drying Technology, 2011. 29(16): p. 1954-1962.
29. Donadon, J.R., et al., *Effect of Hot Air Drying on Ultrastructure of Crambe Seeds.* Drying Technology, 2013. 31(3): p. 269-276.
30. Lewicki, P.P. and G. Pawlak, *Effect of Drying on Microstructure of Plant Tissue.* Drying Technology, 2003. 21(4): p. 657-683.
31. Mazza, G. and M. Lemaguer, *Dehydration of onion: some theoretical and practical considerations.* International Journal of Food Science & Technology, 1980. 15(2): p. 181-194.
32. Suarez, C. and P.E. Viollaz, *Shrinkage effect on drying behavior of potato slabs.* Journal of Food Engineering, 1991. 13(2): p. 103-114.
33. Moreira, R., A. Figueiredo, and A. Sereno, *Shrinkage of apple disks during drying by warm air convection and freeze drying.* Drying Technology, 2000. 18(1-2): p. 279-294.
34. Mayor, L. and A.M. Sereno, *Modelling shrinkage during convective drying of food materials: a review.* Journal of Food Engineering, 2004. 61(3): p. 373-386.
35. Bartlett, M.K., C. Scoffoni, and L. Sack, *The determinants of leaf turgor loss point and prediction of drought tolerance of species and biomes: a global meta-analysis.* Ecology Letters, 2012. 15(5): p. 393-405.

36. Heredia, A., A. Jiménez, and R. Guillén, *Composition of plant cell walls.* Zeitschrift für Lebensmitteluntersuchung und -Forschung A, 1995. 200(1): p. 24-31.
37. Funebo, T., et al., *Microwave heat treatment of apple before air dehydration – effects on physical properties and microstructure.* Journal of Food Engineering, 2000. 46(3): p. 173-182.
38. Monsalve-GonÁLez, A., G.V. Barbosa-CÁNovas, and R.P. Cavalieri, *Mass Transfer and Textural Changes during Processing of Apples by Combined Methods.* Journal of Food Science, 1993. 58(5): p. 1118-1124.
39. Reeve, R.M., *Histological investigations of texture in apples.* Journal of Food Science, 1953. 18(1-6): p. 604-617.
40. Trakoontivakorn, G., M.E. Patterson, and B.G. Swanson, *Scanning electron microscopy of cellular structure of Granny Smith and Red Delicious apples.* Food microstructure, 1988. 7(2): p. 205-212.
41. Khan, A.A. and J.F.V. Vincent, *Anisotropy of apple parenchyma.* Journal of the Science of Food and Agriculture, 1990. 52(4): p. 455-466.
42. Verboven, P., et al., *Three-Dimensional Gas Exchange Pathways in Pome Fruit Characterized by Synchrotron X-Ray Computed Tomography.* Plant Physiology, 2008. 147(2): p. 518-527.
43. Mendoza, F., et al., *Three-dimensional pore space quantification of apple tissue using X-ray computed microtomography.* Planta, 2007. 226(3): p. 559-570.
44. Sterling, C., *Texture and cell wall polysaccharides in foods*, in *Recent Advances in Food Science,* J.M. Leitch, Rhodes, D.N., Editor 1963, Butterworths and Co: London. p. 259-279.
45. Karunasena, H.C.P., et al. *A particle based micromechanics model to simulate drying behaviors of vegetable cells*. in *4th International Conference on Computational Methods (ICCM 2012)*. 2012a. Gold Coast, Australia.

46. Karunasena, H.C.P., et al. *A Coupled SPH-DEM Model for Fluid and Solid Mechanics of Apple Parenchyma Cells During Drying*. in *18th Australian Fluid Mechanics Conference*. 2012b. Launceston - Australia: Australasian Fluid Mechanics Society.
47. Jamaleddine, T.J. and M.B. Ray, *Application of Computational Fluid Dynamics for Simulation of Drying Processes: A Review.* Drying Technology, 2010. 28(2): p. 120-154.
48. Perré, P., *A Review of Modern Computational and Experimental Tools Relevant to the Field of Drying.* Drying Technology, 2011. 29(13): p. 1529-1541.
49. Araujo, J.C., et al., *Comparison of hexamethyldisilazane and critical point drying treatments for SEM analysis of anaerobic biofilms and granular sludge.* Journal of Electron Microscopy, 2003. 52(4): p. 429-433.
50. Bray, D.F., J. Bagu, and P. Koegler, *Comparison of hexamethyldisilazane (HMDS), Peldri II, and critical-point drying methods for scanning electron microscopy of biological specimens.* Microscopy Research and Technique, 1993. 26(6): p. 489-495.
51. Doymaz, İ. and F. Kocayigit, *Drying and Rehydration Behaviors of Convection Drying of Green Peas.* Drying Technology, 2011. 29(11): p. 1273-1282.
52. Ong, S.P. and C.L. Law, *Drying Kinetics and Antioxidant Phytochemicals Retention of Salak Fruit under Different Drying and Pretreatment Conditions.* Drying Technology, 2011. 29(4): p. 429-441.
53. Zhang, F., M. Zhang, and A.S. Mujumdar, *Drying Characteristics and Quality of Restructured Wild Cabbage Chips Processed Using Different Drying Methods.* Drying Technology, 2011. 29(6): p. 682-688.
54. Martin, O., et al., *Food Dehydration*, in *Handbook of Food Engineering, Second Edition*2006, CRC Press. p. 601-744.

55. Wang, C.X., L. Wang, and C.R. Thomas, *Modelling the Mechanical Properties of Single Suspension-Cultured Tomato Cells.* Annals of Botany, 2004. 93(4): p. 443-453.
56. Gao, Q. and R.E. Pitt, *Mechanics of parenchyma tissue based on cell orientation and microstructure.* Transactions of the ASABE, 1991. 34(1): p. 0232-0238.
57. Pitt, R.E., *Models for the Rheology and Statistical Strength of Uniformly Stressed Vegetative Tissue.* Transactions of the ASABE, 1982. 25(6): p. 1776-1784.
58. Taiz, L. and E. Zeiger, *Water and Plant Cells*, in *Plant Physiology*2010, Sinauer Associates. p. 73-84.
59. Nilsson, S.B., C.H. Hertz, and S. Falk, *On the Relation between Turgor Pressure and Tissue Rigidity. II.* Physiologia Plantarum, 1958. 11(4): p. 818-837.
60. Wu, H.-I., et al., *Cell wall elasticity: I. A critique of the bulk elastic modulus approach and an analysis using polymer elastic principles.* Plant, Cell & Environment, 1985. 8(8): p. 563-570.
61. Rahman, M.S., *Toward prediction of porosity in foods during drying: a brief review.* Drying Technology, 2001. 19(1): p. 1-13.
62. Rahman, M., et al., *Thermal Transition Properties of Spaghetti Measured by Differential Scanning Calorimetry (DSC) and Thermal Mechanical Compression Test (TMCT).* Food and Bioprocess Technology, 2011. 4(8): p. 1422-1431.
63. Mohammad Shafi ur, R., *Dehydration and Microstructure*, in *Advances in Food Dehydration*2008, CRC Press. p. 97-122.
64. Karel, M., et al., *Stability-related transitions of amorphous foods.* Thermochimica Acta, 1994. 246(2): p. 249-269.
65. Ratti, C., *Shrinkage during drying of foodstuffs.* Journal of Food Engineering, 1994. 23(1): p. 91-105.

66. Alamar, M.C., et al., *Micromechanical behaviour of apple tissue in tensile and compression tests: Storage conditions and cultivar effect.* Journal of Food Engineering, 2008. 86(3): p. 324-333.

TABLE 1. Cellular geometrical parameter values of different apple cultivars (in fresh condition)

Cultivar	A (μm^2)	D (μm)	P (μm)	R	EL	C	Reference
Golden Delicious	19000 - 45000	100 - 240	540 - 870	0.8	1.6	0.8	Hills et al.[15], Mayor et al.[18]
Delicious	-	160 - 170	-	-	-	-	Reeve [39]
Red Delicious	-	250 - 450	-	-	-	-	Reeve [39]
Idared	10000	100 - 150	470	0.8	-	-	Lewicki and Pawlak [30]
Braeburn	24000 - 32000	150 - 180	570 - 660	1.1	-	1.3	Alamar et al.[66]
Jonagored	24000 - 29000	150 - 170	560 - 630	1.1	-	1.3	Alamar et al.[66]
Smith	-	250 - 450	-	-	-	-	Reeve [39]
Granny Smith	-	-	-	1.2	1.4	-	Bolin and Huxsoll [24]

TABLE 2. Cellular geometrical parameters observed in the 57 ℃ drying experiments

Drying Time (min.)	X/X_0	Cellular Measurements											
		A (μm^2)		D (μm)		P (μm)		R		EL		C	
		avg.	s.d[5] (%)	avg.	s.d (%)	avg.	s.d (%)	avg.	s.d (%)	avg.	s.d (%)	avg.	s.d (%)
0	1.000	21341	40%	164	20%	601	21%	0.727	18%	1.459	17%	0.839	8%
30	0.538	21212	33%	164	16%	576	15%	0.783	10%	1.602	22%	0.805	10%
60	0.216	20151	34%	160	18%	579	21%	0.751	16%	1.591	19%	0.807	10%
90	0.103	18534	40%	153	19%	532	19%	0.794	9%	1.446	18%	0.844	8%
120	0.060	15470	25%	140	13%	505	15%	0.761	14%	1.553	26%	0.827	12%
150	0.025	9760	28%	111	14%	391	14%	0.789	10%	1.582	21%	0.812	10%
180	0.019	9729	41%	111	20%	397	22%	0.760	14%	1.508	21%	0.830	10%
210	0.016	8663	23%	105	11%	377	12%	0.763	13%	1.520	21%	0.828	10%

[5] Standard deviation as a percentage of the corresponding parameter average value

TABLE 3. Cellular geometrical parameters observed in the 70 ℃ drying experiments

Drying Time (min.)	X/X_0	Cellular Measurements											
		A (μm^2)		D (μm)		P (μm)		R		EL		C	
		avg.	s.d (%)	avg.	s.d (%)	avg.	s.d (%)	avg.	s.d (%)	avg.	s.d (%)	avg.	s.d (%)
0	1.000	21341	40%	164	20%	601	21%	0.727	18%	1.459	17%	0.839	8%
30	0.497	19436	32%	157	15%	568	16%	0.741	7%	1.459	14%	0.835	7%
60	0.166	15330	36%	139	17%	486	16%	0.794	11%	1.404	20%	0.858	9%
90	0.085	14634	25%	136	12%	491	14%	0.763	14%	1.397	21%	0.862	9%
120	0.035	12985	36%	128	18%	474	20%	0.715	14%	1.761	27%	0.782	14%
150	0.016	12249	26%	124	12%	446	14%	0.770	10%	1.528	20%	0.823	10%
180	0.015	10454	27%	115	14%	412	17%	0.769	13%	1.433	26%	0.856	11%
210	0.014	8749	33%	105	17%	374	18%	0.769	9%	1.600	23%	0.811	11%

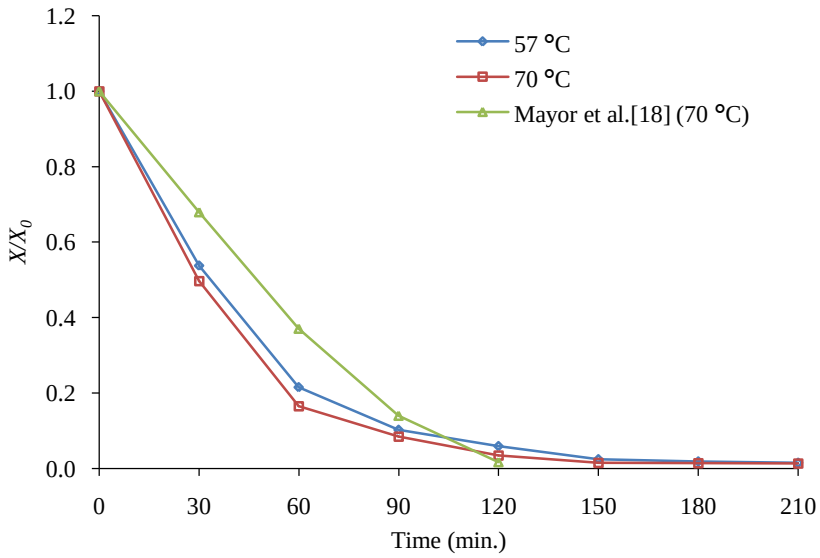

FIG. 1. Drying kinetics of apple slices at 57 ℃ and 70 ℃

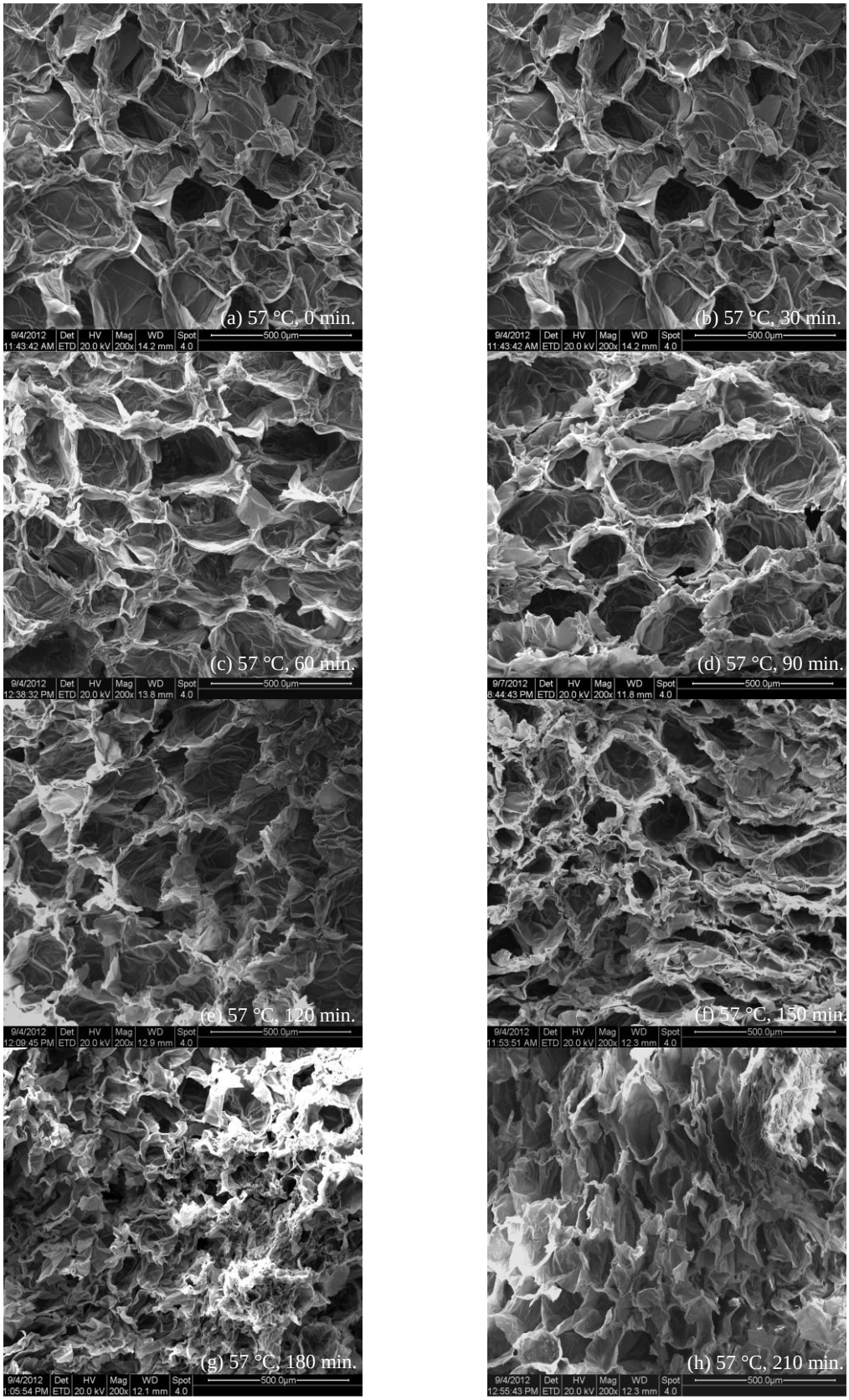

FIG. 2. SEM images of: (a) fresh apple cells; dried cells obtained by drying at 57 ℃ for (b) 30 minutes, (c) 60 minutes, (d) 90 minutes, (e) 120 minutes, (f) 150 minutes, (g) 180 minutes, and (h) 210 minutes.

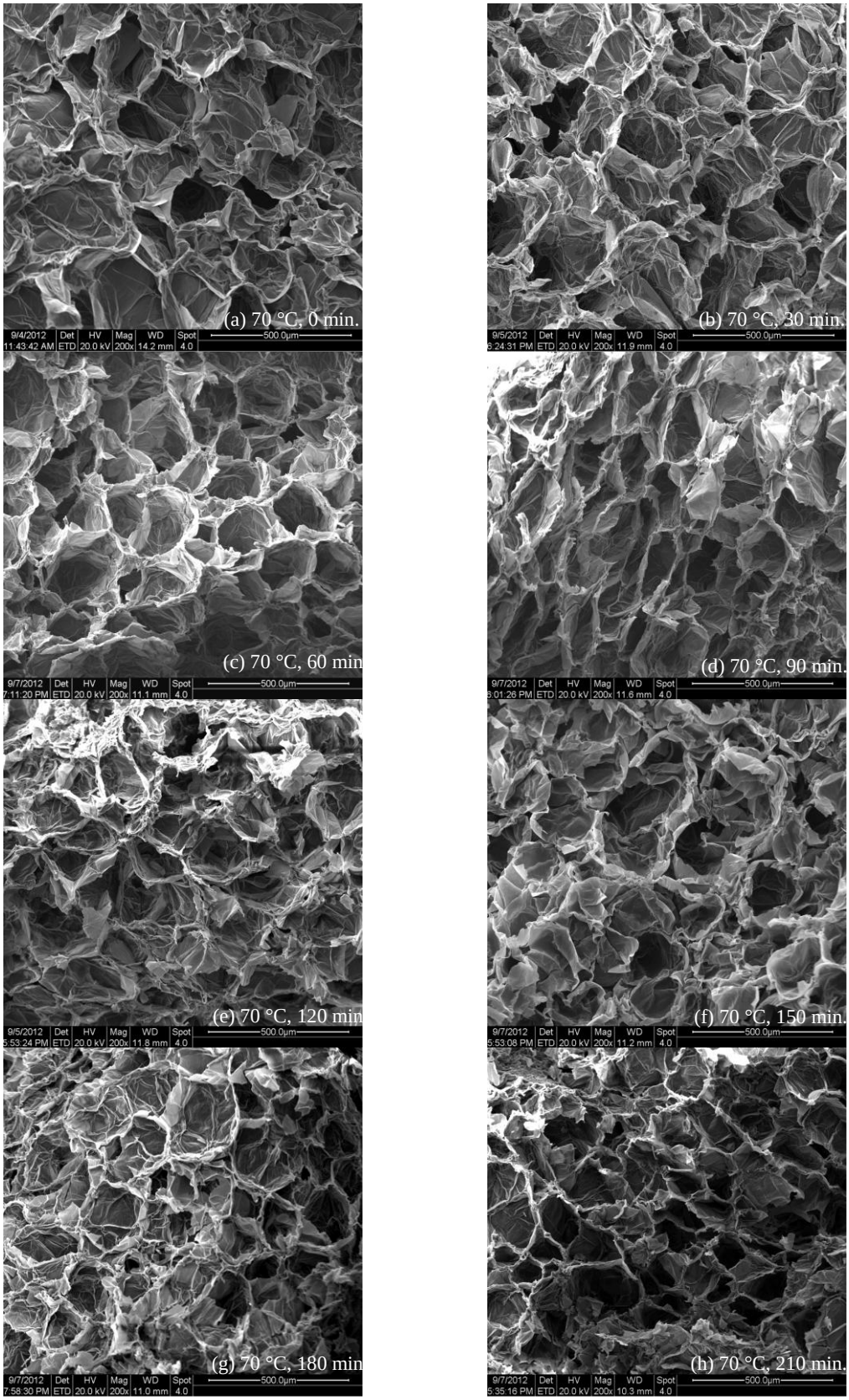

FIG. 3. SEM images of: (a) fresh apple cells; dried cells obtained by drying at 70 °C for (b) 30 minutes; (c) 60 minutes; (d) 90 minutes; (e) 120 minutes; (f) 150 minutes; (g) 180 minutes; (h) 210 minutes.

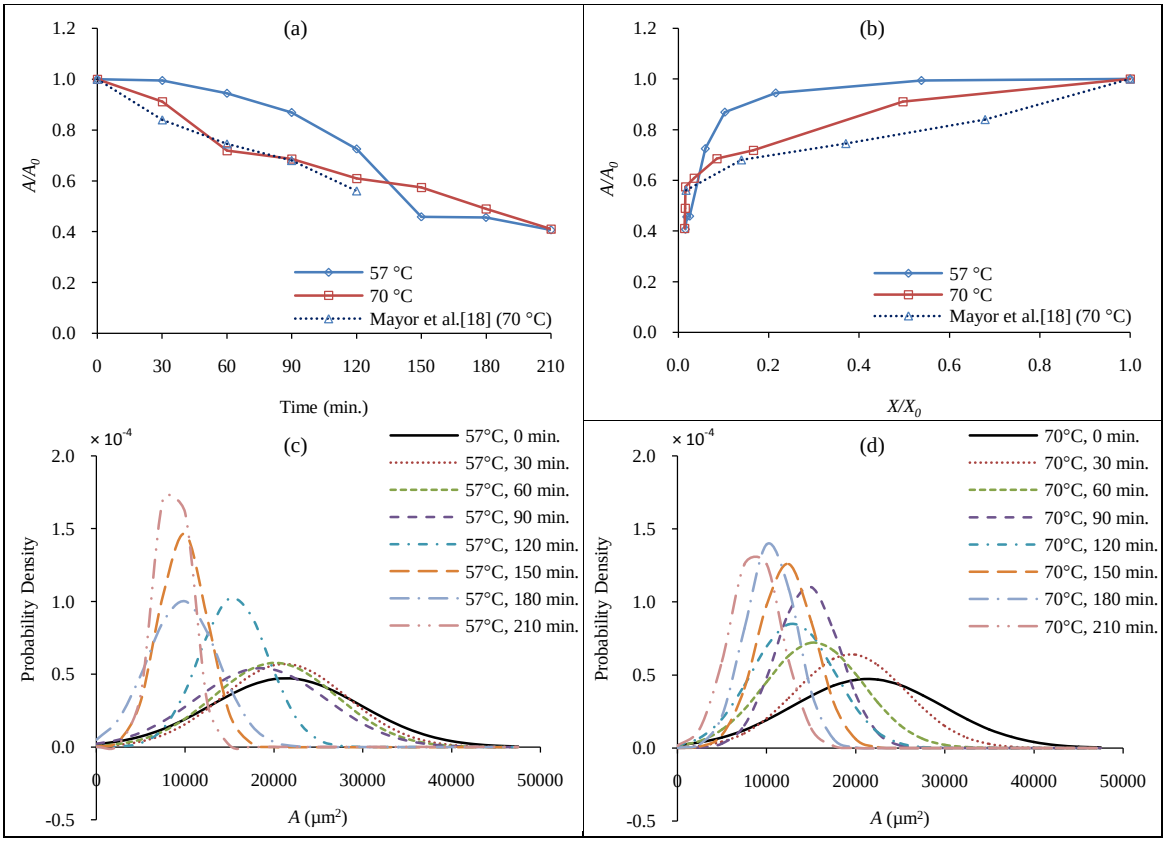

FIG. 4. Cell area characteristics: *(a)* normalized cell area (averaged) vs. time; *(b)* normalized cell area (averaged) vs. normalized moisture content; *(c)* probability density functions (PDFs) of the cell area at different drying times during the 57 ℃ drying experiments; *(d)* PDFs of the cell area at different drying times during the 70 ℃ drying experiments.

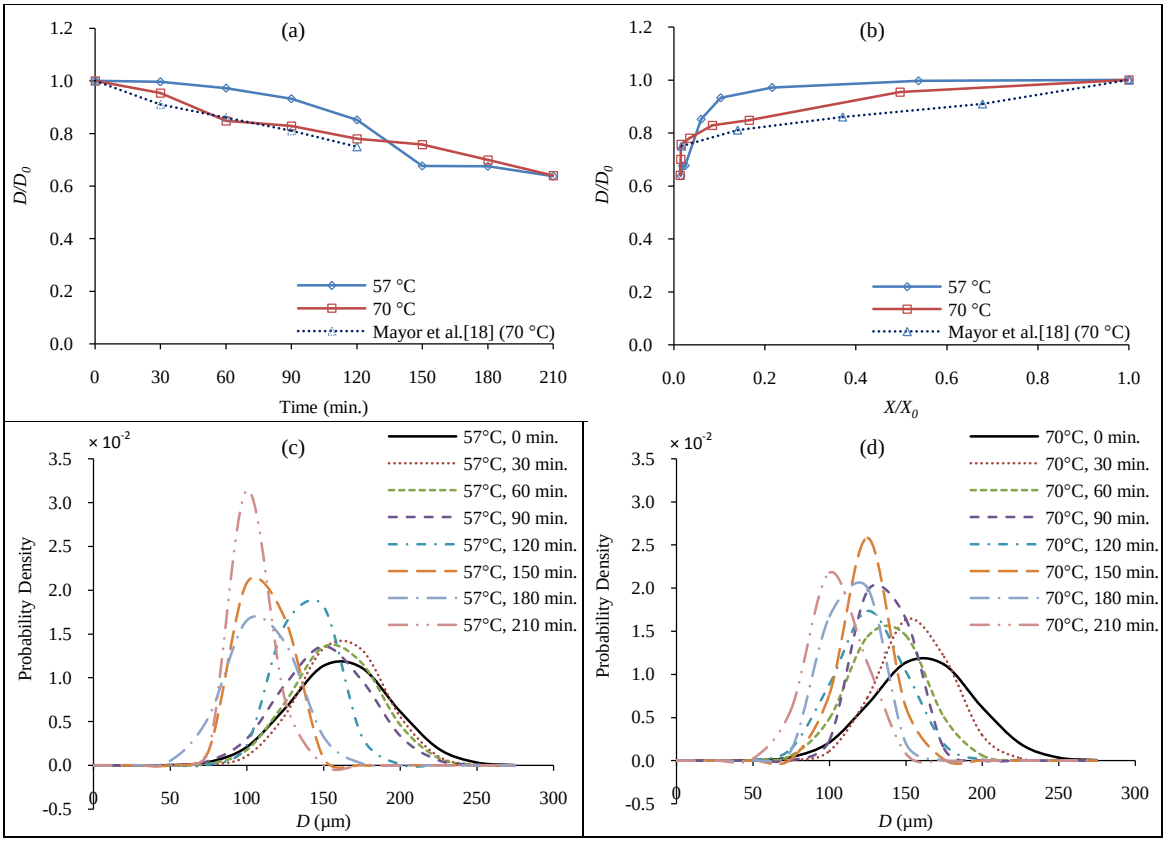

FIG. 5. Cell ferret diameter characteristics: *(a)* normalized cell ferret diameter (averaged) vs. time; *(b)* normalized cell ferret diameter (averaged) vs. normalized moisture content; *(c)* PDFs of the cell ferret diameter at different drying times during the 57 ℃ drying experiments; *(d)* PDFs of the cell ferret diameter at different drying times during the 70 ℃ drying experiments.

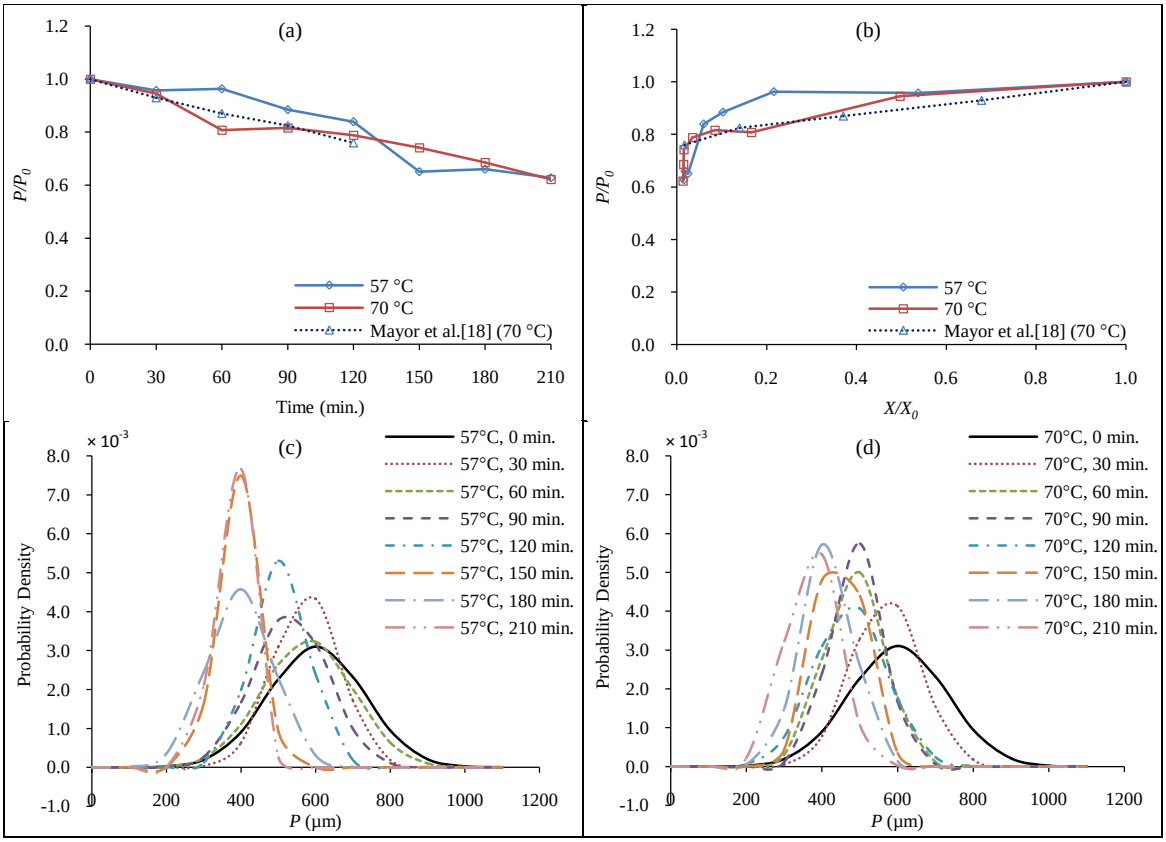

FIG. 6. Cell perimeter characteristics: *(a)* normalized cell perimeter (averaged) vs. time; *(b)* normalized cell perimeter (averaged) vs. normalized moisture content; *(c)* PDFs of the cell perimeter at different drying times during the 57 ℃ drying experiments; *(d)* PDFs of the cell perimeter at different drying times during the 70 ℃ drying experiments.

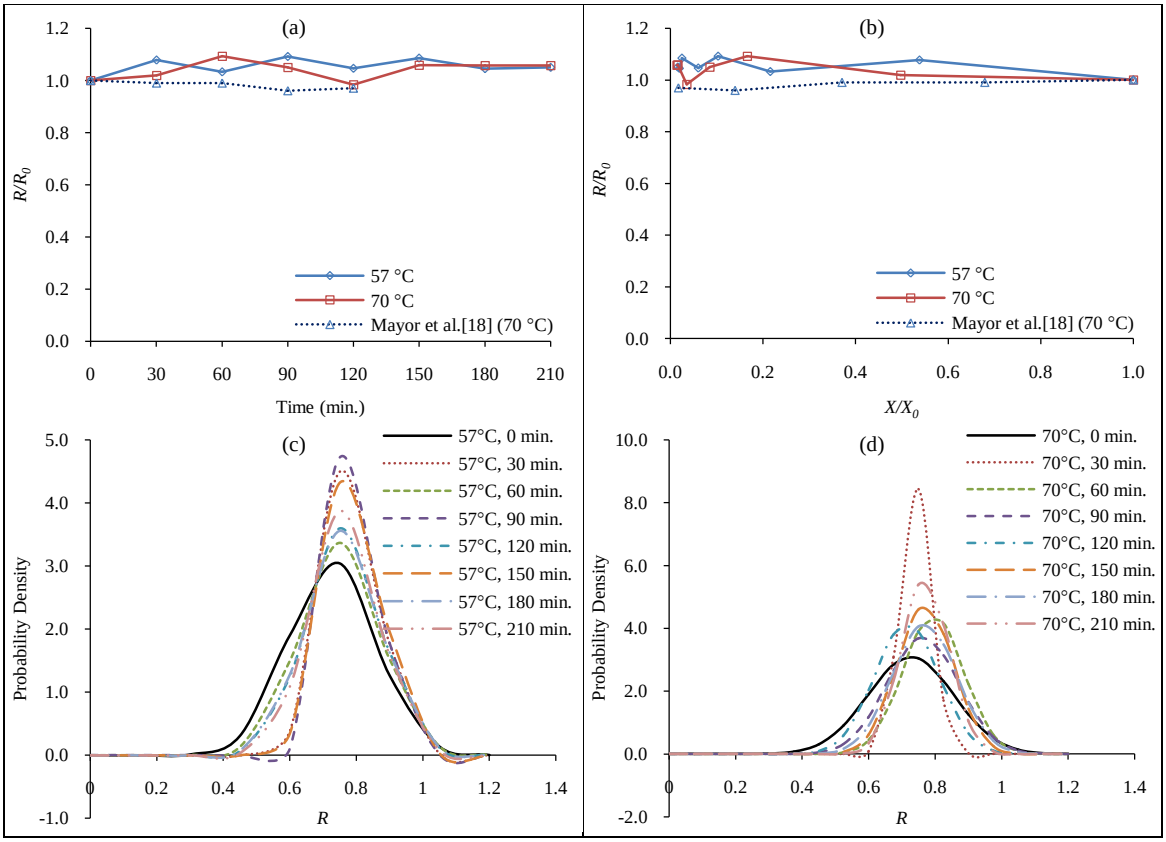

FIG. 7. Cell roundness characteristics: *(a)* normalized cell roundness (averaged) vs. time; *(b)* normalized cell roundness (averaged) vs. normalized moisture content; *(c)* PDFs of the cell roundness at different drying times during the 57 ℃ drying experiments; *(d)* PDFs of the cell roundness at different drying times during the 70 ℃ drying experiments.

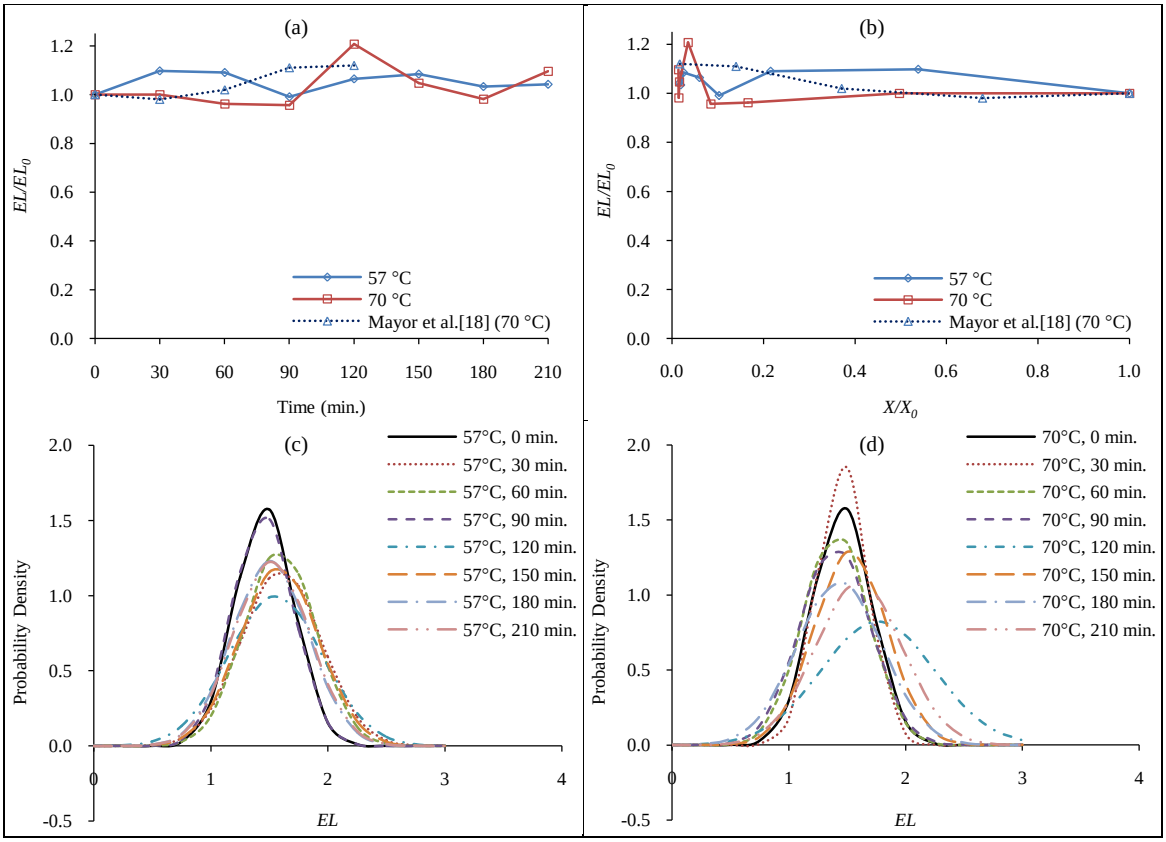

FIG. 8. Cell elongation characteristics: *(a)* normalized cell elongation (averaged) vs. time; *(b)* normalized cell elongation (averaged) vs. normalized moisture content; *(c)* PDFs of the cell elongation at different drying times during the 57 ℃ drying experiments; *(d)* PDFs of the cell elongation at different drying times during the 70 ℃ drying experiments.

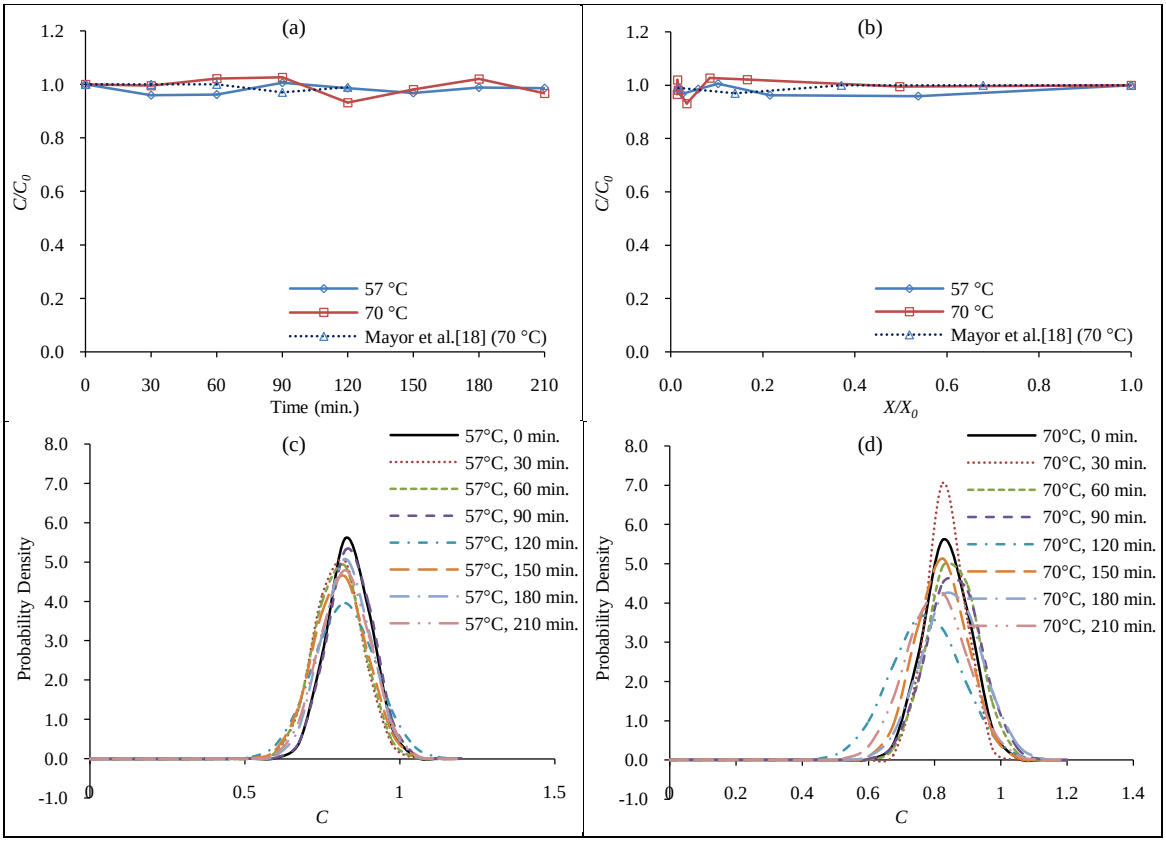

FIG. 9. Cell compactness characteristics: *(a)* normalized cell compactness (averaged) vs. time; *(b)* normalized cell compactness (averaged) vs. normalized moisture content; *(c)* PDFs of the cell compactness at different drying times during the 57 ℃ drying experiments; *(d)* PDFs of the cell compactness at different drying times during the 70 ℃ drying experiments.